Since January 2020 Elsevier has created a COVID-19 resource centre with free information in English and Mandarin on the novel coronavirus COVID-19. The COVID-19 resource centre is hosted on Elsevier Connect, the company's public news and information website.

Analytica Chimica Acta 1219 (2022) 340036

Contents lists available at ScienceDirect

Analytica Chimica Acta

journal homepage: www.elsevier.com/locate/aca

Electromagnetically-driven integrated microfluidic platform using reverse transcription loop-mediated isothermal amplification for detection of severe acute respiratory syndrome coronavirus 2

Yu-Shiuan Tsai [a], Chih-Hung Wang [a], Huey-Pin Tsai [e,f], Yan-Shen Shan [c,d], Gwo-Bin Lee [a,b,*]

[a] Department of Power Mechanical Engineering, National Tsing Hua University, Hsinchu, Taiwan
[b] Institute of NanoEngineering and Microsystems, National Tsing Hua University, Hsinchu, Taiwan
[c] Institute of Clinical Medicine, National Cheng Kung University Hospital, National Cheng Kung University, Tainan, Taiwan
[d] Division of General Surgery, Department of Surgery, National Cheng Kung University Hospital, College of Medicine, National Cheng Kung University, Tainan, Taiwan
[e] Department of Pathology, National Cheng Kung University Hospital, College of Medicine, National Cheng Kung University, Tainan, Taiwan
[f] Department of Medical Laboratory Science and Biotechnology, College of Medicine, National Cheng Kung University, Tainan, Taiwan

HIGHLIGHTS

- Rapid and accurate diagnosis of severe acute respiratory syndrome coronavirus 2 (SARS-CoV-2) was reported.
- An electromagnetically-driven microfluidic chip was developed to lyse viruses, extract their RNAs, and perform qualitative analysis of three marker genes by on-chip RT-LAMP within 82 min.

GRAPHICAL ABSTRACT

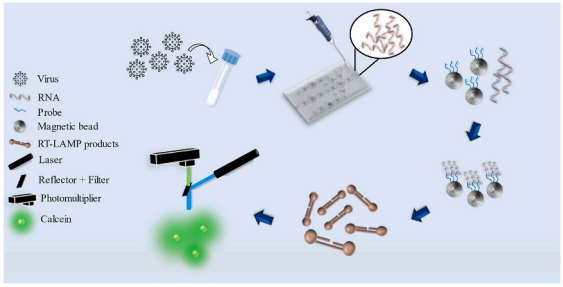

ARTICLE INFO

Keywords:
COVID-19
Microfluidics
Multiple RT-LAMP
Micropumps
Micromixers
Point-of-care

ABSTRACT

Rapid, sensitive and accurate diagnosis of severe acute respiratory syndrome coronavirus 2 (SARS-CoV-2) is of great need for effective quarantining and treatment. Real-time reverse-transcription polymerase chain reaction requiring thermocyling has been commonly used for diagnosis of SARS-CoV-2 though it may take two to 4 h before lengthy sample pretreatment process and require bulky apparatus and well-trained personnel. Since multiple reverse transcription loop-mediated isothermal amplification (multiple RT-LAMP) process without thermocycling is sensitive, specific and fast, an electromagnetically-driven microfluidic chip (EMC) was developed herein to lyse SARS-CoV-2 viruses, extract their RNAs, and perform qualitative analysis of three marker genes by on-chip multiple RT-LAMP in an automatic format within 82 min at a limit of detection of only ~5000 copies per reaction (i.e. 200 virus/ μL). This compact EMC may be especially promising for SARS-CoV-2 diagnostics in resource-limited countries.

* Corresponding author. Department of Power Mechanical Engineering, National Tsing Hua University, Hsinchu, 30013, Taiwan.
E-mail address: gwobin@pme.nthu.edu.tw (G.-B. Lee).

https://doi.org/10.1016/j.aca.2022.340036
Received 28 December 2021; Received in revised form 2 June 2022; Accepted 2 June 2022
Available online 6 June 2022

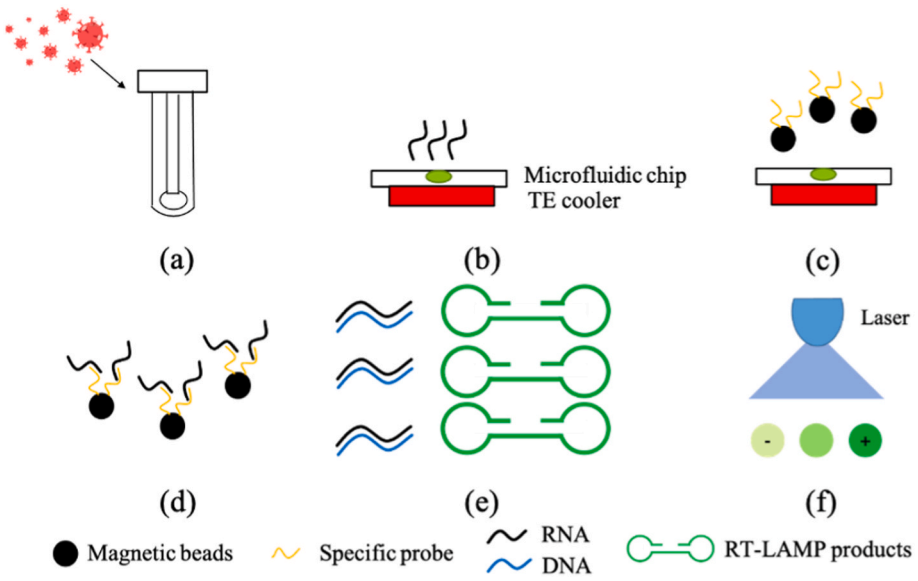

Fig. 1. Schematic of the experimental procedure; (a) viral swab sample collection and chip loading to the platform; (b) virus lysis while the swab sample has been loaded into the chip; (c) addition of magnetic beads coated with specific probes into the chip for (d) RNA extraction, (e) LAMP amplification with reverse transcription carried out simultaneously, and subsequent (f) fluorescence detection to distinguish the positive and negative results. TE = thermoelectric.

1. Introduction

Severe acute respiratory syndrome coronavirus 2 (SARS-CoV-2) is responsible for the 2019 coronavirus (COVID-19) pandemic [1]. SARS-CoV-2 is an RNA virus and belongs to the betacoronavirus subfamily of the coronavirinae family [2]; its viral characteristics are now under extensive investigation [3,4]. According to the World Health Organization, the incubation period from initial infection to onset of symptoms is 1–14 days (mostly 5–6 days) [5], indicating that fast, sensitive and accurate diagnosis plays an important role in quarantining and planning effective treatment.

Nucleic acid amplification technology is an important tool in pathogen diagnostics [6,7]. In addition to the commonly used polymerase chain reaction (PCR), nucleic acid sequence-based amplification [8] and self-sustained sequence replication [9] have been used, but they all require thermal cycling, lengthy reaction times (up to 2 h or even 4 h), and bulky and expensive equipment [10]. Furthermore, they requires well-trained personnel to operate the diagnostic process. Alternatively, loop-mediated isothermal amplification (LAMP) does not require thermocycling and simply constant incubation at 60–65 °C for 30–60 min could be used for LAMP [11]; this allows for the use of more compact, field-ready devices when compared to conventional PCR; reverse transcription loop-mediated isothermal amplification (RT-LAMP) can be even carried out in remote locations by those with minimal training for RNA-based pathogens (such as SARS-CoV-2). Furthermore, after the termination of the reaction, magnesium pyrophosphate is commonly used to induce precipitation [12], and SYBR® Green [13], hydroxy naphthol blue (HNB) [14], or phenol red [15] can be used as proxies for reaction success confirmation (typically as presence/absence) [16].

Recently, a variety of microfluidic devices and systems have been demonstrated for viral detection [17–23] via reverse transcription PCR (RT-PCR) and other means. For instance, RT-PCR has been used in diagnosis of SARS-CoV-2 using microfluidic techniques [24], and microfluidics-based, nL-scale PCR could be performed successfully with a limit of detection (LOD) of 1000 copies within 210 min. In one example [25], both the Orf1ab and N genes could be detected within 75 min at an LOD of 10^4 copies mL^{-1}. Similarly, a centrifugal microfluidic platform featuring real-time PCR could detect 2×10^4 copies mL^{-1} of the SARS-CoV-2 N gene without RNA extraction within 90 min [26]. Note that most of the above-mentioned devices only deal with on-chip nucleic acid amplification, not tedious sample pretreatment processes such as lysis and RNA extraction.

Alternatively, RT-LAMP has been used in SARS-CoV-2 diagnostics as well, including a smartphone-controlled method whose LOD for the Orf1ab gene was 10^4 copies mL^{-1} in 60 min [27]. Similarly, a centrifugal microfluidic device with visual detection was demonstrated [28], and the polystyrene toner-based microfluidic device reported a LOD of 1 copy mL^{-1} via on-chip SYBR Green intercalation; a handheld ultraviolet source connected to a smartphone also realized quantification of the viruses [28]. Furthermore, a rapid, isothermal portable detection system [29] for SARS-CoV-2 was characterized by an LOD of 5×10^4 copies mL^{-1} (N gene) in 30 min without on-chip RNA extraction. Even though these devices have shown promise, none are capable of undertaking the entire process including virus lysis, RNA extraction, and RT-LAMP on the same device; the need for off-chip processing increases the possibility of contamination and requires well-trained personnel, which may hinder their applications. Furthermore, most RT-PCR and RT-LAMP assays for detection of SARS-CoV-2 [24–29] focus on only 1–2 genes, even though a three-gene approach featuring RdRp, E, and N genes (preferably detected simultaneously) [30] would reduce both false-positive and false-negative diagnoses [36]. In this work, an electromagnetic microfluidic chip (EMC) adopted from our previous work [31] equipped with micropumps and micromixers was modified to be equipped a new detachable "magnetic structure layer" herein to control samples and reagents. Moreover, micro temperature control and optical detection modules were further integrated with the electromagnetically-driven microfluidic devices to detect all three genes (RdRp, E, and N) of SARS-CoV-2 in parallel optically on a single chip that could carry out all steps of the viral gene detection process (Fig. 1) while integrating new on-chip RT-LAMP devices. Furthermore, three RNA probes were designed to capture three target RNAs such that they could be efficiently captured by magnetic beads. Moreover, three sets of LAMP primers were designed to amplify three target genes specifically. The performance of the developed microfluidic system were characterized with synthesized complementary DNA (cDNA), synthesized RNAs, inactive viruses, and RNA extracted from virus samples. To the best of our knowledge, it is the first time that an electromagnetically-driven microfluidic system was used for automatic, parallel detection of three genes of SARS-CoV-2 using RT-LAMP.

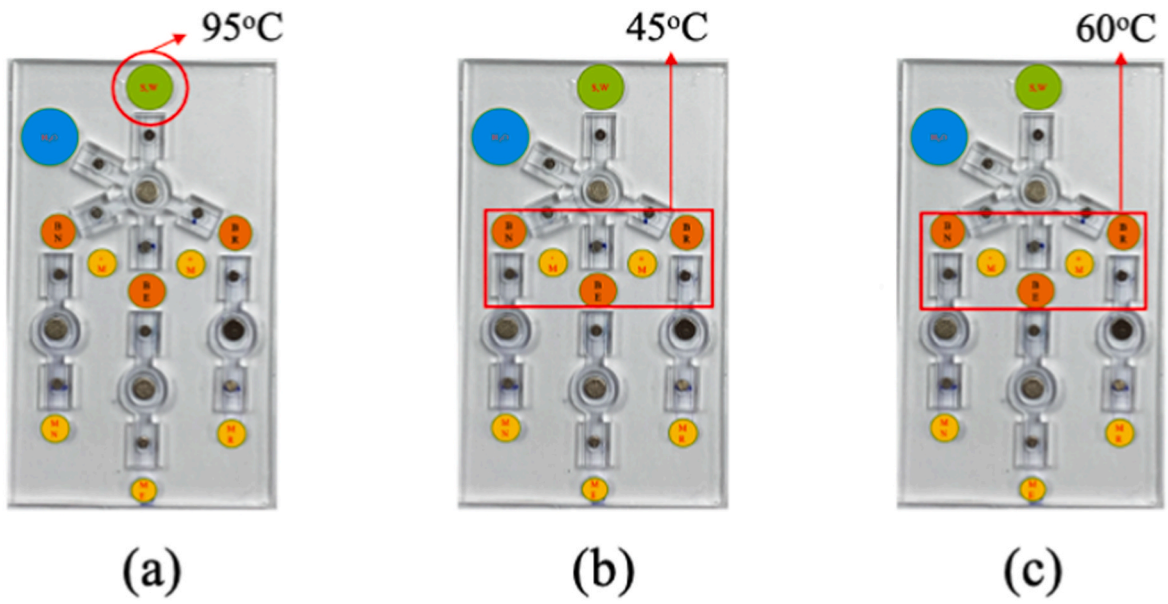

Fig. 2. A schematic of the on-chip procedure post-loading of the chambers. (a) Lysis (95 °C for 5 min) to release RNAs from viruses (or chemical lysis at room temperature for 20 min). (b) Magnetic beads were added into the chip for capturing RNAs for three genes at 45 °C for 10 min. (c) RT-LAMP at 60 °C for 60 min.

2. Materials and methods

2.1. Experimental procedure

A schematic illustration of the SARS-CoV-2 detection procedure is shown in Fig. 1a–f. Briefly, samples (synthesized RNAs, synthesized cDNA, inactive viruses (concentration = 10^4 copies μL^{-1}, 15 μL; Qnostics, UK) or RNAs extracted from virus samples), viral RNA lysis buffer (R145; ABP Biosciences, USA), wash buffer (nuclease-free water; 300 μL), MyOneTM carboxylic acid magnetic Dynabeads (10^5 beads μL^{-1}, 5 μL, 1.05 μm in diameter; Invitrogen, USA) for capture of RdRp, E, and N genes (5 μL per chamber; 10^{13} copies μL^{-1}; synthesized RNAs for positive controls purchased from Antech Diagnostics, USA), and RT-LAMP mastermix (Tables S1–S2; 24 μL per chamber) were added to the respective chambers of the EMC (Fig. 1a). Prior to analysis, the magnetic beads were coated with RNA probes (amine group modification) (Table S3) by carboxylation with 1-Ethyl-3-(3-Dimethylaminopropyl) carbodiimide catalytic action [31]. Note that these three RNA probes were specifically designed to be complementary to three target genes (i.e. RdRp, E, and N genes) such that they could be used to capture them efficiently. For inactive viruses, they were lysed (Fig. 2a) chemically at room temperature for 20 min using the lysis buffer (90 μL) or thermally at 95 °C for 5 min in chamber C1 (Figs. 2a and S4) by a thermoelectric (TE) cooler (TEC1-241.10, Tande, Taiwan). Next, RNA samples (including released RNA from inactive viruses, synthesized RNA or RNA extracted from real viruses provided from National Cheng Kung University Hospital, Taiwan [NCKUH]; 100 μL of 10^8 copies μL^{-1}) were divided into three equal volumes and transported to chambers C3, C5, and C7 (Fig. S4), and RNA extraction (Fig. 2b) was carried out via magnetic beads at 45 °C (Fig. 2b) for 10 min. Then, three electromagnets that were placed above the three chambers containing the magnetic beads were used to mix samples with beads by turning the electromagnets on and off sequentially. After washing with water, electromagnets placed underneath each chamber enabled collection of

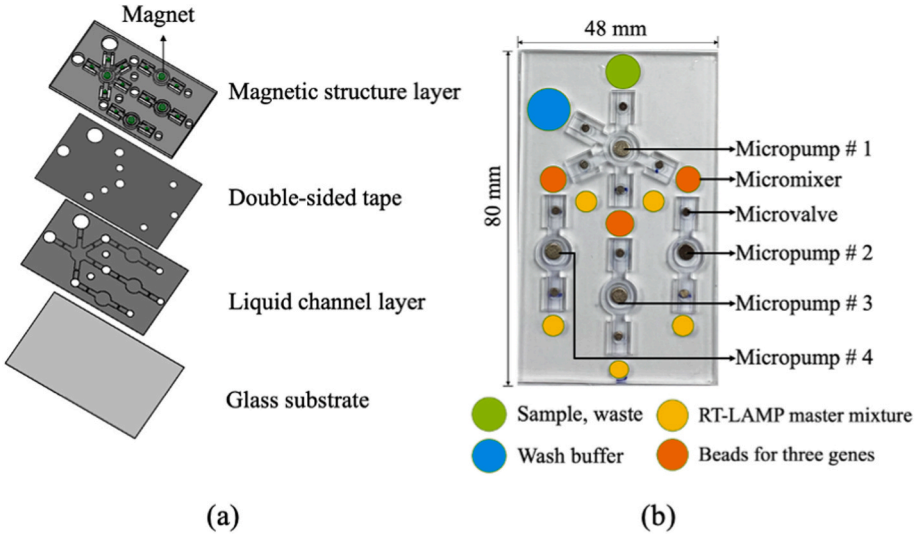

Fig. 3. (a) An exposed view of the electromagnetically-driven microfluidic chip. (b) A schematic illustration depicting the 11 microvalves, 4 micropumps, 10 loading chambers (for samples & reagents), washing buffer chamber, and waste reservoir.

RNA-bead complexes (Fig. 1d). Afterwards, mastermixes from chambers C8, C9, and C10 (Fig. S4) were transported to reaction chambers C3, C5, and C7, respectively, to perform RT-LAMP at 60 °C for 60 min (Fig. 1e & 2c). Forward outer primer (F3), backward outer primer (B3), forward inner primer (FIP) and backward inner primer (BIP) were used (Table S2), and dumbbell-shaped RT-LAMP products were produced. Note that these primers were specifically designed to amplify three target genes via LAMP. Finally, fluorescent detection was used for qualitative analysis after RT-LAMP (Fig. 1f); in contrast to our prior works with SYBR Green [32], 0.5 mM calcein (10 μL; C0875, Sigma, USA) with $MnCl_2$; (2.5 μL; 13446-34-9, Sigma) was used for fluorescent detection. Detailed information about the chip layout can be found in Figs. S4 and a detailed, on-chip actuation protocol for the thermal lysis (82 min totally) or chemical lysis (97 min totally) procedure can be found in Table S4.

2.2. Design and microfabrication of the EMC

The 48 × 80 × 3 mm EMC (Fig. 3a–b) was composed of a magnetic structure layer, a double-side-tape layer, a liquid channel layer, and a glass substrate (0.4 mm, Ruilong Optoelectronics, Taiwan) (Fig. 3a). The former was used to align detachable magnets with the corresponding electromagnets placed underneath, and the liquid channel layer was for sample and reagent transport. Microstructures were designed by AutoCAD 2019 and Solidworks 2014, and the EMC was microfabricated by casting of polydimethylsiloxane (PDMS; 12:1 A:B ratio) onto polymethyl methacrylate (PMMA) mastermolds (Figs. S5–S6) as in a prior work [31]. To align the permanent magnets, they were first fixed on a PMMA mold, and PDMS was then poured over the mold to position them above the top PDMS layer. The magnetic structure layer was then bonded to the liquid channel layer by the double-sided tape; finally, all layers were bonded on the glass substrate. The EMC (Fig. S4) was composed of microvalves (2.6 mm in width and 9 mm in depth), micropumps (6 mm × 7 mm), 10 loading chambers (for samples & reagents), a wash buffer chamber (0.2 mm × 0.2 mm), and a waste reservoir (3 mm × 3 mm). The widths of chambers for samples, three kinds of magnetic beads (for RdRp, E, & N genes, respectively), RT-LAMP mastermix, positive, and negative controls were all 5 mm except for the former (7 mm; all depths were 3 mm). Permanent magnets (diameter & thickness = 2 mm × 1 mm for the microvalve magnet & 4 mm × 1 mm for the micropump magnet; Powerful Magnets, Taiwan) were inserted in the magnetic structure layer (Fig. 3b) to deflect the PDMS membranes and thereby electromagnetically activate the microvalves, micromixers, and micropumps [31] via a handmade electromagnet made of an iron core (500-coil turns). It is worth noting that when compared with our prior design [31], the detachable magnetic structure layer in this work allowed this compact device to be reusable, and the 12:1 PDMS ratio resulted in a softer PDMS membrane that could be more readily deflected. Since the micromixers were activated via the electromagnet, they could be reused as well.

2.3. Experimental setup

The system (Fig. S7) was composed of fluid control (Fig. S9), temperature control (Fig. S3), and optical detection modules (Fig. S8). To activate the device electromagnetically (Fig. S1), an Arduino mega controller (Italy) compiled the codes for controlling the electronic components, and a power supply (CPS-3205 II, Hundred Years Electronic, Taiwan) activated the flow control module at 8–10 V. Nine direct0-current (DC) motor bridges (L298n, STMicroelectronics, China) controlled the 18 electromagnets that then controlled the microvalves, micromixers, and micropumps. The temperature control module was composed of the aforementioned TE coolers, a copper plate with a tunnel to place a thermocouple (Scientific Center, National Tsing Hua University, 7.3 mm × 7.3 mm x 3.0 mm & 40.0 mm × 18.0 mm x 3.0 mm) for feedback control, two relays (JQC-3FF-S-Z, Hundred Years

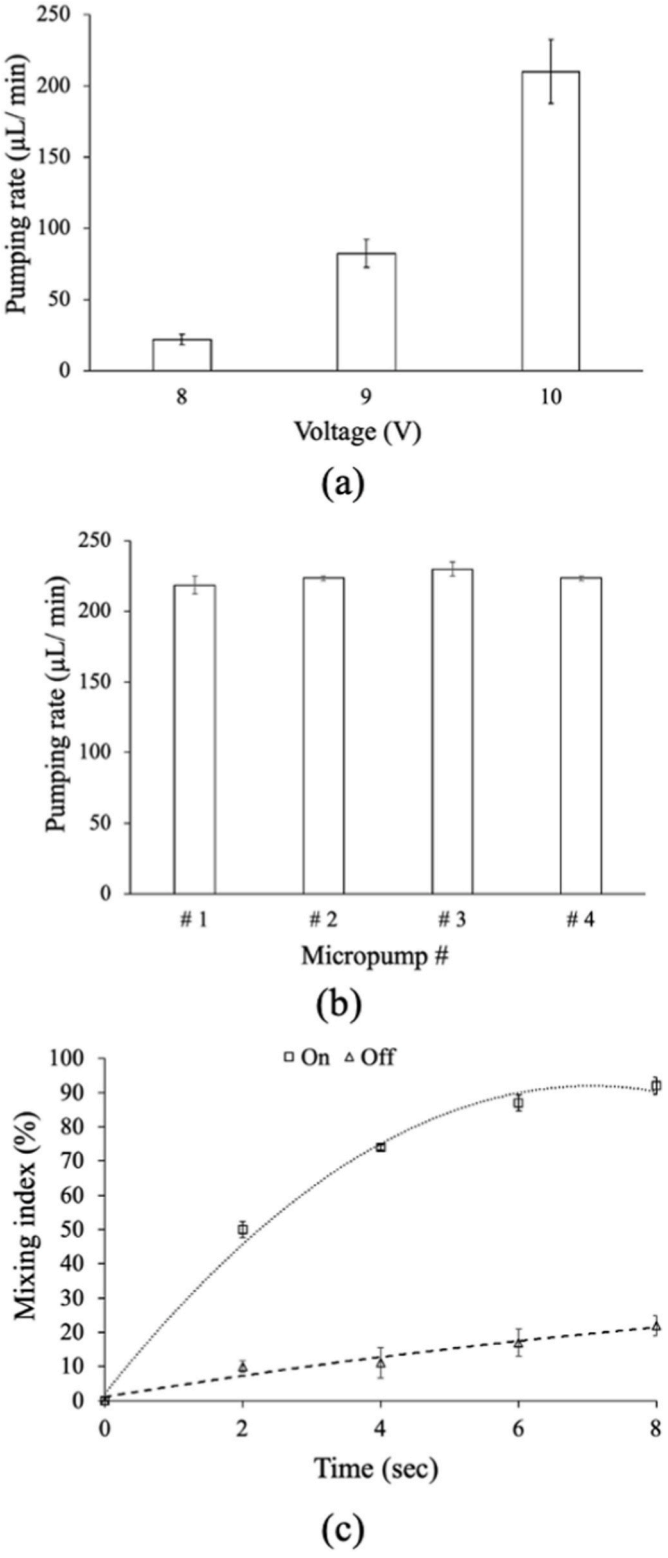

Fig. 4. (a) Pumping rates of the electromagnetically-driven micropumps at three electromagnet voltages. (b) Pumping rates of four micropumps at 10 V and 0.5 Hz. (c) Mixing index of the electromagnetically-driven micromixer at 10 V and 0.5 Hz. In all panels, error terms reflect standard error of the mean (n = 3).

Electronic Inc.) controlled by the Arduino Uno controller (itself integrated with a computer), and another thermocouple (Max6675, Hundred Years Electronic; Fig. S10) placed in the chamber to calibrate the real temperature of liquid in the chamber before carrying out RT-LAMP. Then the temperature of the copper plate was compensated to tune in the temperature of liquid in the chamber precisely. Finally, the thermocouple in the chamber was removed and then RT-LAMP was carried out automatically. Once the temperature reached the target value, the relays cut off the power to stop heating. Note that the temperature control module was placed underneath the microfluidic chip such that the required temperature control could be precisely regulated. The optical detection module (Fig. S8) was composed of a photomultiplier tube (PMT; C6271, Hamamatsu Photonics, Japan) for collecting fluorescence signals, a laser (MBL–III–473, Changchun New Industries Optoelectronics, China) for exciting calcein from RT-LAMP products by using blue light (495 nm), a reflector (T495LP, Mirle, China) for reflecting the excited light from the light source to the sample, an optical filter (525 nm, ET525, Chroma ATE, Taiwan), an objective lens (U47365, Onset Electro-optics, Taiwan), and a computer for data analysis. Photographs of the flow control/temperature control modules for the multiple RT-LAMP system (Fig. S11(a)) and the optical detection module (Fig. S11 (b)) could be found in Supplementary Information. Note that these three modules could be integrated into a box with dimensions of 45 cm × 30 cm x 30 cm (length x width x height) (Fig. S11(c)).

2.4. Sample preparation

Four samples were used, including synthesized RNAs containing three genes, synthesized cDNA containing three genes, inactive viruses of SARS-CoV-2 and extracted RNA samples from virus samples. The inactive viruses of SARS-CoV-2 was purchased from Qnostics Ltd., Scotland, UK (concentration = 10^4 copies μL^{-1}, 500 μL); the synthesized RNAs for three genes was purchased from Antech Diagnostics, California, USA (Concentration of RNAs = 10^{13} copies μL^{-1}, 40 μL); synthesized cDNA was produced by synthesized RNAs by reverse transcription. Extracted RNA samples of virus samples was obtained from NCKUH (Original type, concentration of RNAs = 10^8 copies μL^{-1}, 100 μL). These protocols were carried out in accordance with the guidelines and regulations from NCKUH.

2.5. Statistical analysis

The fluorescence intensity of serially diluted samples were compared with the negative control among triple experiments in this study. Therefore, the two-tailed student *t*-test analysis was used to calculate whether there was a significant difference ($p < 0.05$) for LOD determination.

3. Results and discussion

3.1. Characterization of micropumps, micromixers, and TE coolers

Since the micropump was activated via electromagnets since they could defect the PDMS membranes to push liquid underneath (Fig. S1), the optimal voltage (8, 9, or 10 V) for liquid transport was first explored with water for 30 s at 0.5 Hz (Fig. 4a); even though transport (i.e. pumping rate = pumping volume/time, pumping volume: volume of transported liquid) scaled linearly and positively with voltage, we did not increase the voltage beyond 10 V to avoid damaging the EMC's components. As such, 10 V was used for subsequent experiments, including micropump characterization; Furthermore, for four micropumps on the chip (as shown in Fig. 3b), their pumping rates were measured to be 218.4 ± 6.3, 223.4 ± 1.5, 229.8 ± 5.1, and 223.4 ± 1.5 μL min^{-1} at 0.5 Hz (Fig. 4b); this is sufficient for liquid transport. The low degree of variation also highlights the uniform distribution of reagents/samples throughout the EMC.

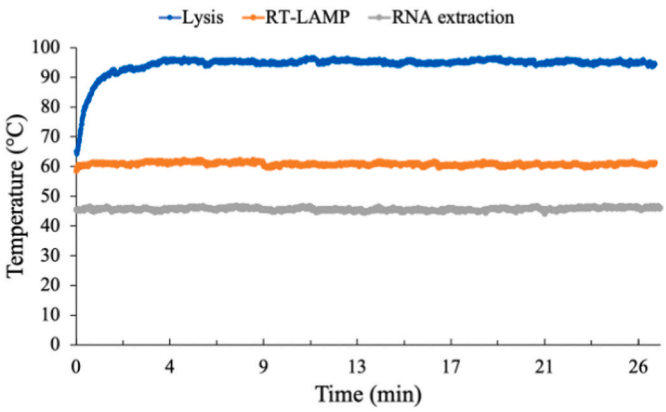

Fig. 5. Temperature profiles over time for thermal lysis, RNA extraction, and RT-LAMP by using two thermoelectric (TE) coolers.

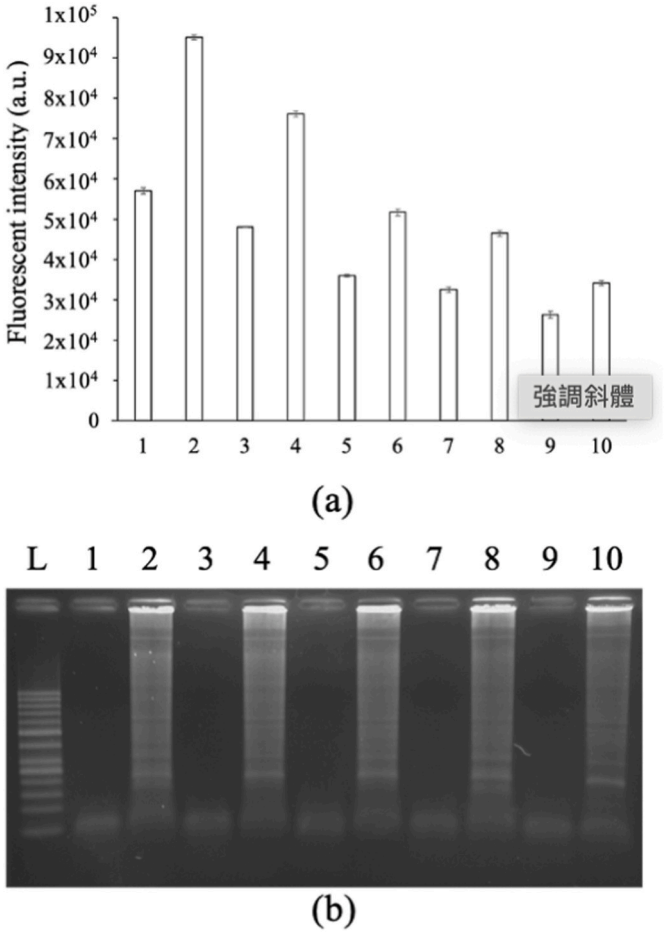

Fig. 6. Optimizing the calcein dosage. (a) Fluorescent detection with an ELISA reader (error bars = standard error of the mean [n = 3]) and (b) agarose gel electrophoresis of five different calcein solutions: 0.5 mM calcein was added to 5 (lanes 1–2), 7.5 (lanes 3–4), 10 (lanes 5–6), 12.5 (lanes 7–8), and 15 mM $MnCl_2$ (lanes 9–10). L: 50-bp DNA ladder; Lanes 1, 3, 5, 7, 9: negative control (water); Lanes 2, 4, 6, 8, 10: RdRp gene.

These constituents were mixed via the electromagnetically-driven micromixer (Fig. S2) after using water and dye to estimate the mixing index as in a prior work [33]. As shown in Fig. 4c, the mixing index reached 92% within 8 s at 10 V and 0.5 Hz (4-fold higher than when the mixer was not used), indicating that the micromixer could be efficient to mix samples and reagents.

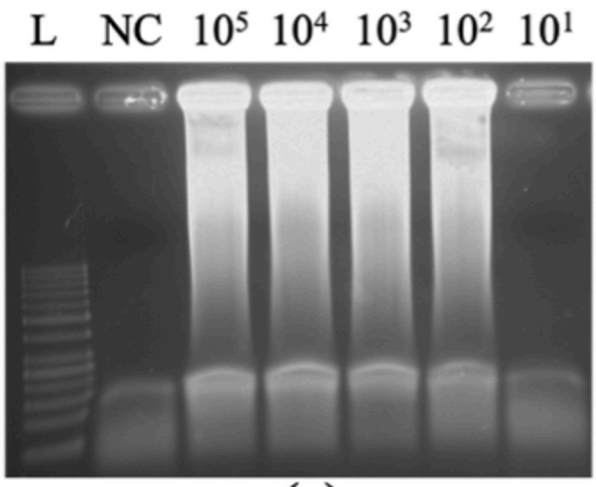

(a)

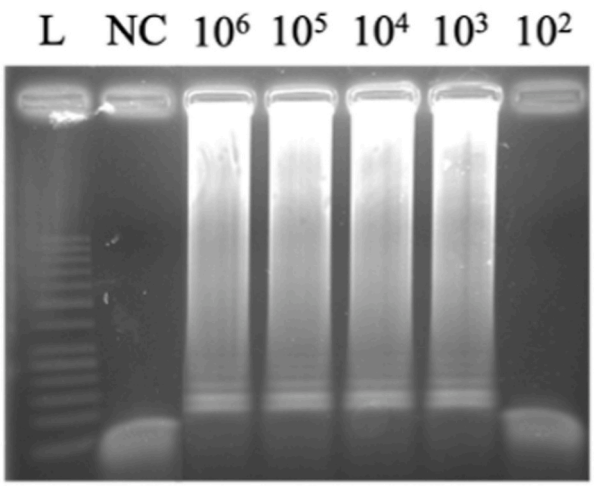

(b)

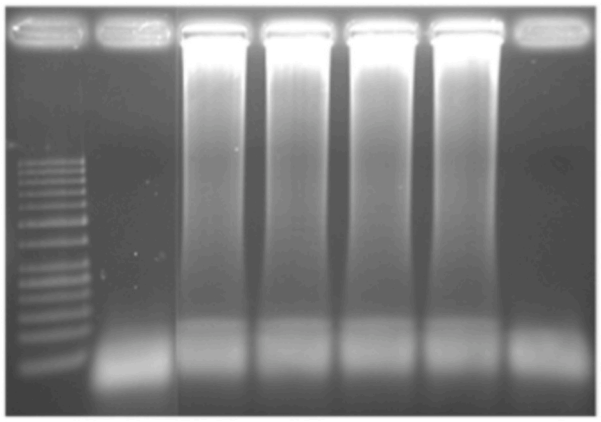

(c)

Fig. 7. LAMP sensitivity tests which were carried out on-chip using cDNA from the (a) RdRp, (b) E, and (c) N genes for 60 min. L: 50-bp DNA ladder, NC: Negative control (water), Lanes 10^6 to 10^1: copies per reaction of each gene.

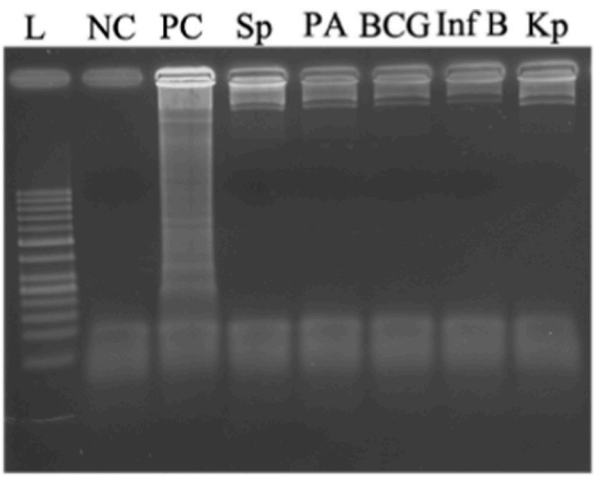

(a)

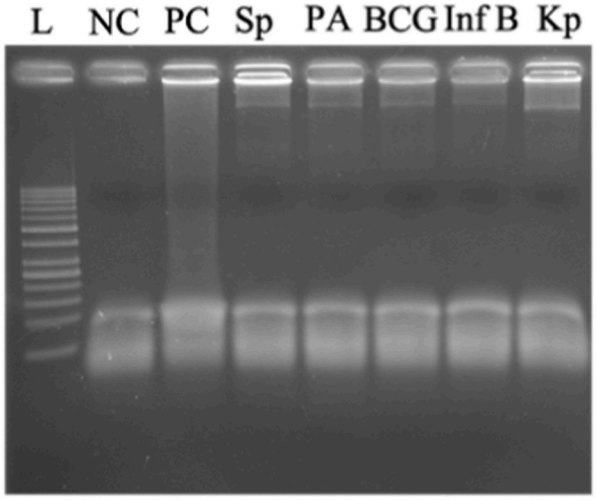

(b)

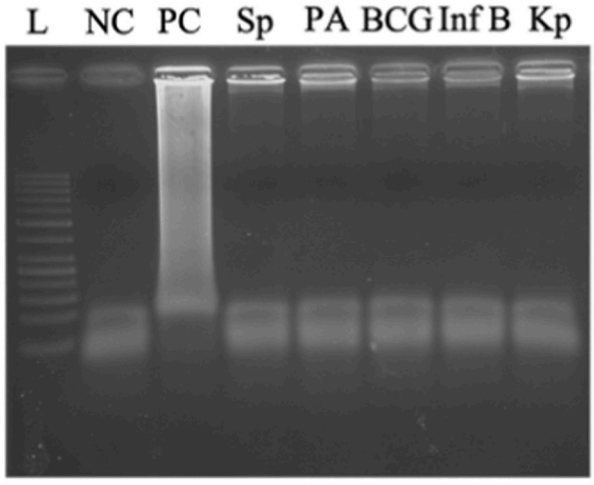

(c)

Fig. 8. Specificity tests with cDNA which were carried out on-chip. (a) RdRp, (b) N gene, and (c) N gene with cDNA for 60 min. L: 50-bp DNA ladder, NC: Negative control (water), PC: Positive control (1000 copies per reaction for each gene), Sp: *Streptococcus pneumoniae*, PA: *Pseudomonas aeruginosa*, BCG: *Mycobacterium bovis*, Inf B: *Influenza B*, Kp: *Klebsiella pneumonia* (10^{11} copies per reaction for all microbes).

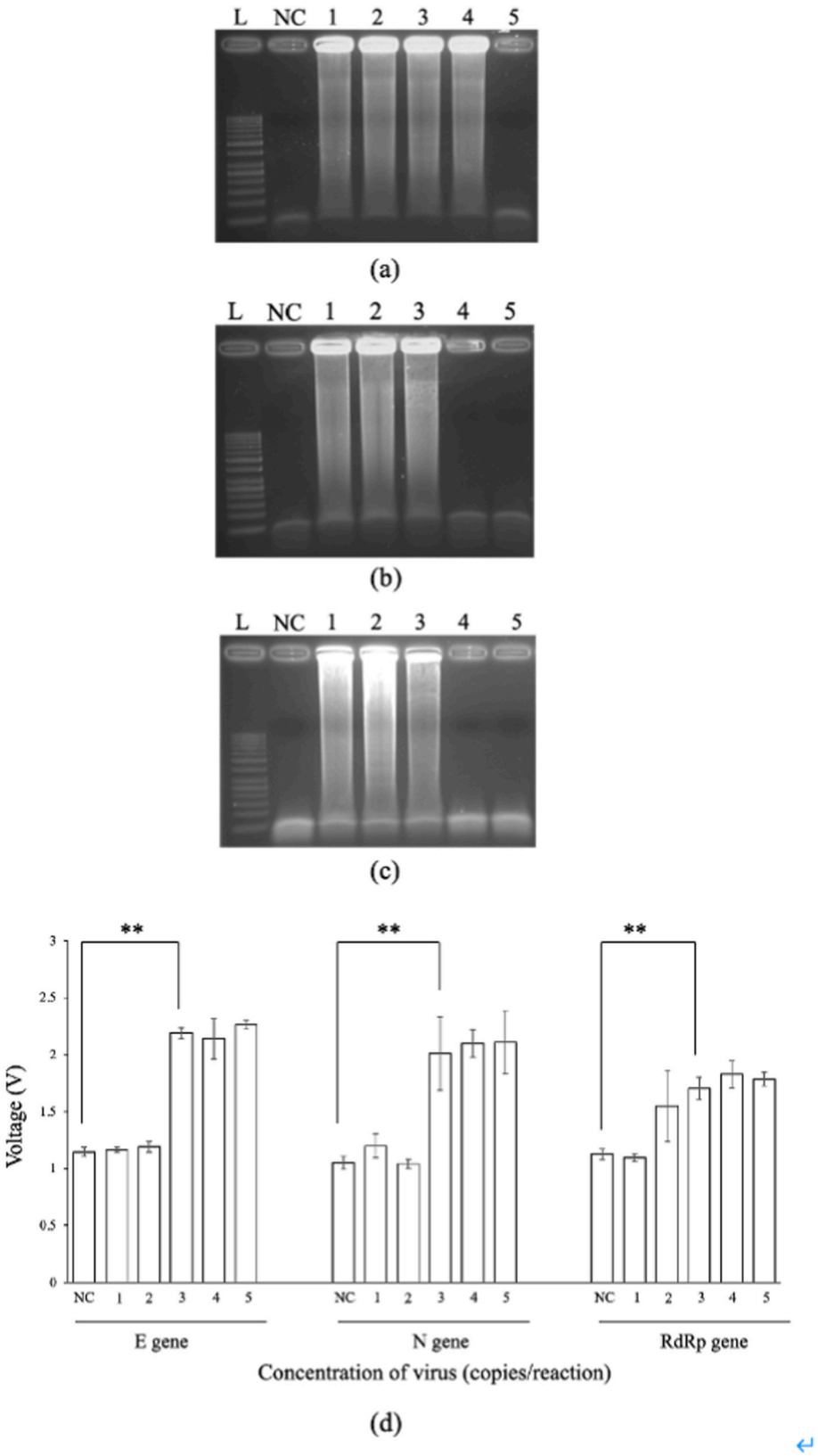

Fig. 9. Sensitivity tests for on-chip RNA extraction + RT-LAMP using synthesized RNAs for the (a) RdRp, (b) E, and (c) N genes. L: 50-bp DNA ladder; NC: Negative control (water); Lanes 1 to 5: 5×10^5 to 50 copies per reaction, respectively. Error bars represent standard error of the mean (n = 3). ** was indicated as $p < 0.05$ by two-tailed student *t*-test analysis.

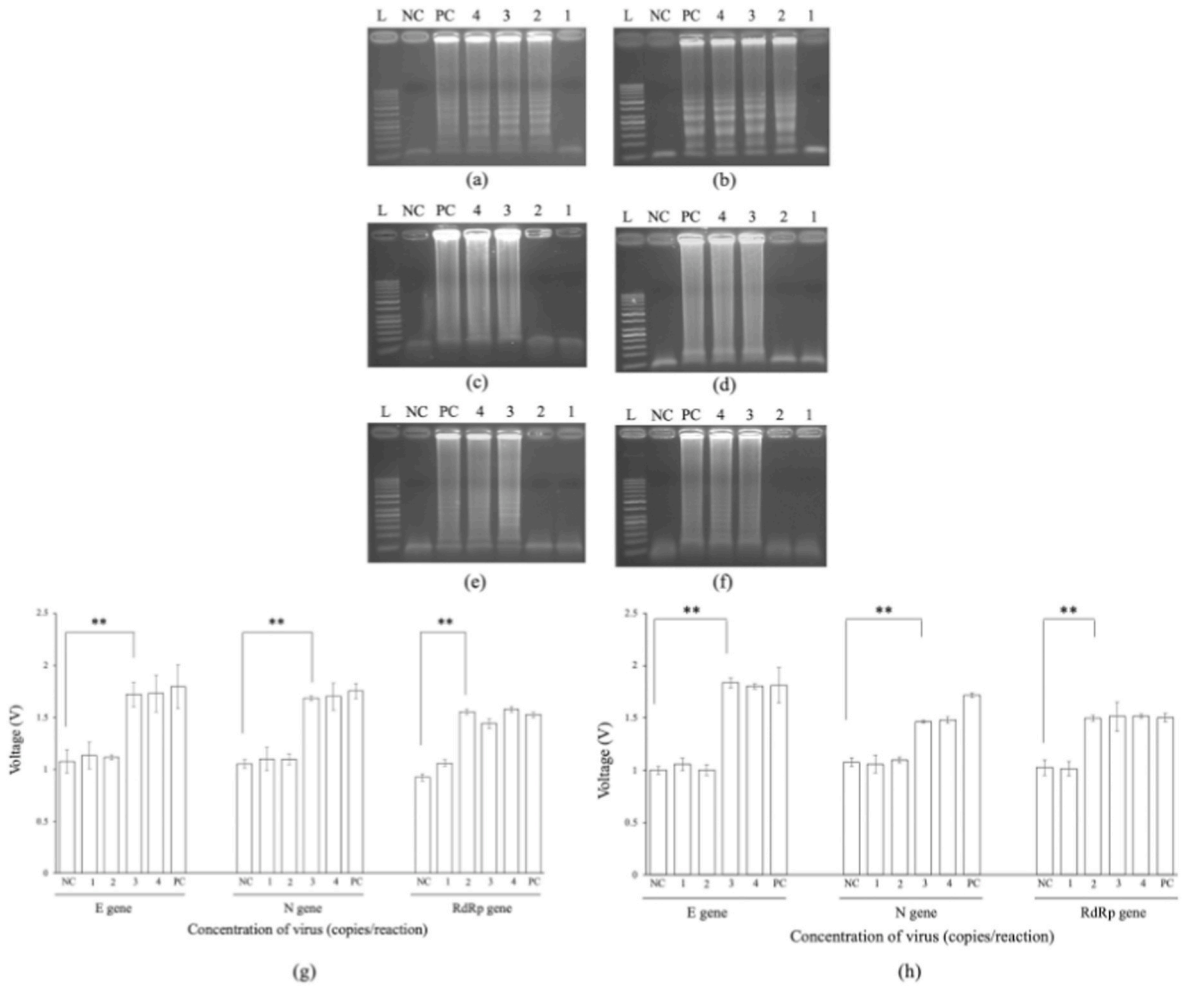

Fig. 10. Sensitivity tests for on-chip RNA extraction + RT-LAMP using inactive viruses for the (a) RdRp, (b) E, and (c) N genes. L: 50-bp DNA ladder; NC: Negative control (water); Lanes 1 to 5: 5×10^5 to 50 copies per reaction, respectively. Error bars represent standard error of the mean (n = 3). ** was indicated as $p < 0.05$ by two-tailed student *t*-test analysis.

In this work, two TE coolers were used for temperature control (Fig. S3). Experimental results show that samples reached 95 °C (±0.5 °C) within 100 s via the first TE cooler. The second TE cooler was used for RNA extraction and RT-LAMP (Fig. 5) at 60 and 45 °C, respectively (±0.5 °C for each). The accurate temperature control attributes to a feedback control from two thermocouples located in a temperature control module placed underneath the microfluidic chip such that two TE coolers could provide required temperature profiles.

3.2. Optimization of concentrated calcein solution

To titrate the optimal ratio of calcein/$MnCl_2$ to quantify the LAMP products (Fig. 6), various concentrations of the latter were mixed with 0.5 mM calcein with the solutions tested with both positive (10^5 copies per reaction of RdRp) and negative controls (water); In order to distinguish the positive/negative results clearly, the largest positive vs. negative fluorescent signal differential was achieved by using an enzyme-linked immunosorbent assay (ELISA) reader (POLARstar Omega, BMG Labtech, Germany) at 0.5 mM calcein+5 mM $MnCl_2$ (Fig. 6a); this result was corroborated via gel electrophoresis (Fig. 6b). It should be noted that the operating principle of fluorescence detection with the calcein solution is to use $MnCl_2$ to block fluorescence from calcein. However, in order to get the optimized calcein solution, several ratios of calcein/$MnCl_2$ were tested to make the positive and negative results more distinguishable. The background signal may be reduced from adding more $MnCl_2$; however, it might result in a weak positive result which cannot be distinguished clearly. Finally, the optimized ratio of the calcein solution was decided accordingly (as shown in Fig. 6).

3.3. On-chip LAMP sensitivity and specificity tests using synthesized cDNA

In order to ensure that LAMP could be performed optimally in the EMC, cDNAs reverse-transcribed from the RdRp, E, and N genes were tested at concentrations ranging from 10 to 10^6 copies per reaction for 60-min LAMP (Fig. 7a–c), and the LODs were found to be 10^3 copies per reaction for the latter two; the RdRp LOD (Fig. 7a) was only 100 copies per reaction. The polymerase may have lost activity for the other genes, though 1000 copies per reaction is an acceptable LOD for LAMP, and values are often higher as reported in previous works (e.g., 10^4 copies per reaction) [32].

The specificity of the LAMP assay is also superior to that of PCR since more than two primers are used for LAMP [11]. In this work, four primers were used, and we tested their ability to amplify genes from other common acute upper respiratory viruses and bacteria: *Streptococcus pneumoniae*, *Pseudomonas aeruginosa*, *Mycobacterium bovis*, *Influenza B*, *Klebsiella pneumonia* (10^{11} copies per reaction for each). As shown in Fig. 8a–c, only genes of the target virus, SARS-CoV-2, were detected (even at only 1000 copies per reaction), indicating that the primers are specific for the target virus.

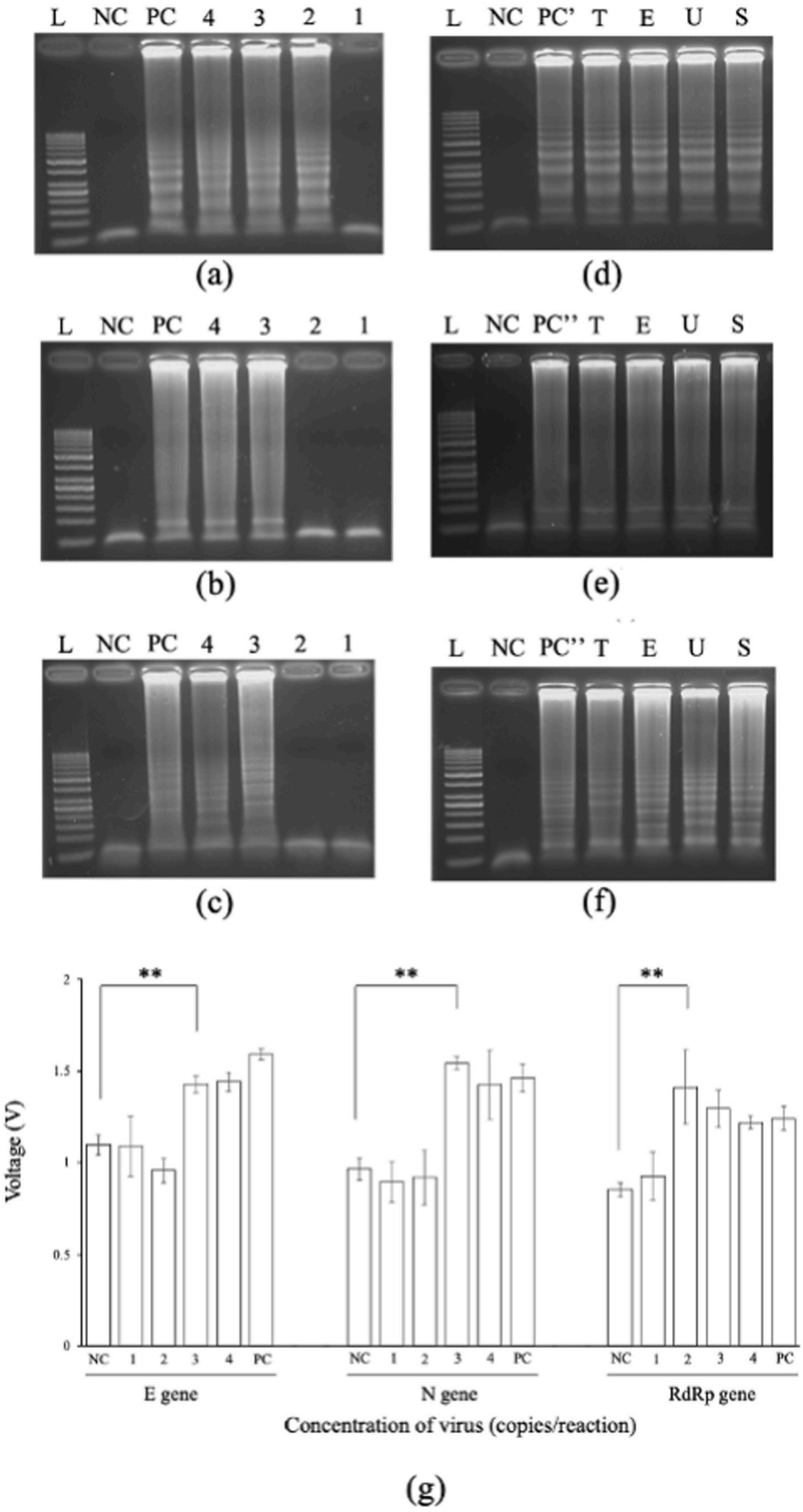

Fig. 11. Sensitivity tests for on-chip RNA extraction + RT-LAMP with RNA extracted from virus samples for (a,d) RdRp, (b,e) E, and (c,f) N genes. (g) Fluorescence detection after RT-LAMP for three genes. Error bars represent standard error of the mean (n = 3). L: 50-bp DNA ladder; NC: Negative control (water); PC: Positive control (5×10^4 copies per reaction of synthesized RNAs); PC': 500 copies per reaction; PC'': 5000 copies per reaction; Lanes 4 to 1: 5×10^4 to 50 copies per reaction, respectively; T, E, U, and S=SARS-CoV-2 viruses sourced from Taiwan, England, USA, and Spain, respectively. ** was indicated as $p < 0.05$ by two-tailed student *t*-test analysis.

3.4. On-chip RT-LAMP sensitivity tests using synthesized RNAs

To simulate that viral RNAs were released into solution, 5 μL of synthesized RNAs (10^5 copies μL^{-1}) were spiked into 30 μL of water and then captured by 5 μL of magnetic beads (10^6 beads μL^{-1}) surface-coated with specific RNA probes (Fig. 9a–c). Then, RT-LAMP were carried out to explore the sensitivity of the developed assay. The LOD was found to be 5×10^3 copies per reaction after RNA extraction + RT-LAMP for the E and N genes and only 500 copies per reaction for RdRp. When using the optical detection module (Fig. 9d), results were similar to those of gel electrophoresis (5×10^3 copies per reaction). These results suggest that the EMC can successfully detect RNA viruses via RT-LAMP and subsequent fluorescence detection by using the optical detection module.

3.5. Sensitivity tests with inactive viruses and virus samples

Inactive SARS-CoV-2 viruses were tested on-chip (Fig. 10a–h), and both chemical and thermal lysis were found to be effective for viral lysis (97 & 82 min, respectively). The LOD of RdRp was found to be ~500 copies per reaction (5000 for the other genes), and the fluorescent results corroborated this gel-based finding (Fig. 10g–h).

The LODs were the same when analyzing SARS-COV-2 RNAs (with an initial concentration of 10^8 copies μL^{-1}) extracted from viruses (Fig. 11a–h). Experimental results show that even at 5000 copies per reaction, these LODs, which were corroborated by fluorescence detection (Fig. 11g), are superior to those of a prior work [34]: 10^4 copies per reaction. Other works did obtain lower LODs for the N gene alone (1.25×10^3 copies per reaction [32,35]), though our device could detect three genes simultaneously. Furthermore, our RdRp LOD is superior, and we tested the assay successfully with RNA samples extracted from viruses from four countries (Taiwan, England, USA, and Spain) (Fig. 11d–f), demonstrating the bio-applicability of the developed system.

As mentioned earlier, several methods for detection of SARS-CoV-2 have been developed recently [24–30]. However, only one to two genes were detected in these studies and it might compromise of the accuracy of the tests. According to a previous study [36], the false negative rate (FNR) was explored by using PCR with three genes and FNR was found to be down to 9.3% which was lower than the one with only one or two genes (i.e. 30%) [37]. It indicates that not only did the multiple RT-LAMP of three genes reduce the test time but it also lowered the FNR. Regarding the LOD, a previous work [35] showed that SARS-CoV-2 viruses were tested with clinical specimens, including bronchoalveolar lavage fluid (n = 15), fibrobronchoscope brush biopsies (n = 13), sputum (n = 104), nasal swabs (n = 8), pharyngeal swabs (n = 398), feces (n = 153), blood (n = 307), and urine (n = 72). The mean threshold values for all were $>2.6 \times 10^4$ copies per reaction except for nasal swabs (1.4×10^6 copies per reaction). Therefore, the LOD reported in this work is considered sufficient for clinical tests [35]. Note that all modules were integrated together and it could be carried with easy such that it could be used as a point-of-care device if necessary. On the contrary, the other previous works [35–37] required either a PCR machine or an ELISA reader, which are not easy to be carried for on-site applications. Besides, the whole procedure were not automated on their platforms since sample pretreatment or optical analysis was carried out off chip.

It should be noted that all experiments were carried out by using inactive viruses (in Fig. 10) or RNAs extracted from virus samples (in Fig. 11). These results can verify that the reusable part (i.e. top layer with permanent magnets) worked and was not contaminated since it was not in contact with any sample.

4. Conclusions

In summary, a new electromagnetically-driven integrated microfluidic platform was developed to automate the entire diagnostic process of SARS-CoV-2 viruses. Virus lysis, RNA extraction, RT-LAMP and optical detection procedure could be performed automatically. It can quickly extract viral RNAs and quantify viral gene concentrations via RT-LAMP and optical detection; only 5000 copies of viral RNAs could be detected, indicating that this device could be a promising, rapid, and affordable tool for COVID-19 diagnostics.

CRediT authorship contribution statement

Yu-Shiuan Tsai: conceived, designed, and conducted the experiments, performed the experiments, Writing – original draft, All authors contributed scientific discourse, commented on the manuscript, and approved its final incarnation. **Chih-Hung Wang:** conceived, designed, and conducted the experiments, prepared the biological samples and performed the statistical analysis, All authors contributed scientific discourse, commented on the manuscript, and approved its final incarnation. **Huey-Pin Tsai:** collected RNA specimens, Writing – original draft, All authors contributed scientific discourse, commented on the manuscript, and approved its final incarnation. **Yan-Shen Shan:** collected RNA specimens, All authors contributed scientific discourse, commented on the manuscript, and approved its final incarnation. **Gwo-Bin Lee:** Writing – original draft, conceived, designed, and conducted the experiments. All authors contributed scientific discourse, commented on the manuscript, and approved its final incarnation.

Declaration of competing interest

The authors declare that they have no known competing financial interests or personal relationships that could have appeared to influence the work reported in this paper.

Acknowledgements

The authors thank the Ministry of Science and Technology (MOST) of Taiwan for funding this work (MOST 109B0247J3; 109-2224-E-007-002; 109-3114-Y-001-001; 109Q22803E1; 110Q2804E1). Partial financial support from the National Health Research Institutes of Taiwan (NHRI-EX110-11020EI) is greatly appreciated.

Appendix A. Supplementary data

Supplementary data to this article can be found online at https://doi.org/10.1016/j.aca.2022.340036.

References

[1] C. Chen, COVID-19 pandemic, Int. Surg. J. 104 (2019), 89-89.
[2] C.P. Czerny, Corona viruses-A pathogenically variable family, Tierärztliche Umsch. 49 (1994) 511–515.
[3] P. Lio, N. Goldman, Phylogenomics and bioinformatics of SARS-CoV, Trends Microbiol. 12 (2004) 106–111.
[4] M. Hasoksuz, S. Kilic, F. Sarac, Coronaviruses and SARS-COV-2, Turk. J. Med. Sci. 50 (2020) 549–556.
[5] T.H. Li, H.Z. Lu, W.H. Zhang, Clinical observation and management of COVID-19 patients, Emerg. microbes & infect. 9 (2020) 687–690.
[6] Y.J. Chen, C. Qian, C.Z. Liu, H. Shen, Z.J. Wang, J.F. P, J. Wu, H. Chen, Nucleic acid amplification free biosensors for pathogen detection, Biosens. Bioelectron. 153 (2020) 1–17.
[7] J.D. Fox, Nucleic acid amplification testes for detection of respiratory viruses, J. Clin. Virol. 40 (2007) S15–S23.
[8] B. Deiman, P. van Aarle, P. Sillekens, Characteristics and applications of nucleic acid sequence-based amplification, Mol. Biotechnol. 20 (2002) 163–179.
[9] J.D. Mueller, B. Putz, H. Hofler, Self-sustained sequence replication (3SR): an alternative to PCR, Histochem. Cell Biol. 108 (1997) 431–437.
[10] M. Inaba, Y. Higashimoto, Y. Toyama, T. Horiguchi, M. Hibino, M. Iwata, K. Imaizumi, Y. Doi, Diagnostic accuracy of LAMP versus PCR over the course of SARS-CoV-2 infection, Int. J. Infect. Dis. 107 (2021) 195–200.
[11] T. Notomi, H. Okayama, H. Masubuchi, T. Yonekawa, K. Watanabe, N. Amino, T. Hase, Loop-mediated isothermal amplification of DNA, Nucleic Acids Res. 28 (2000) 1–7.
[12] Y. Mori, K. Nagamine, N. Tomita, T. Notomi, Detection of loop-mediated isothermal amplification reaction by turbidity derived from magnesium pyrophosphate formation, Biochem. Biophys. Res. Commun. 289 (2001) 150–154.

[13] T. Iwamoto, T. Sonobe, K. Hayashi, Loop-mediated isothermal amplification for direct detection of Mycobacterium tuberculosis complex, M-avium, and M-intracellulare in sputum samples, J. Clin. Microbiol. 41 (2003) 2616–2622.
[14] M. Goto, E. Honda, A. Ogura, A. Nomoto, K.I. Hanaki, Colorimetric detection of loop-mediated isothermal amplification reaction by using hydroxy naphthol blue, Biotechniques 46 (2009) 167–172.
[15] C.B. Poole, Z.R. Li, A. Alhassan, D. Guelig, S. Diesburg, N.A. Tanner, Y.H. Zhang, T. C. Evans, P. LaBarre, S. Wanji, R.A. Burton, C.K.S. Carlow, Colorimetric tests for diagnosis of filarial infection and vector surveillance using non-instrumented nucleic acid loop-mediated isothermal amplification (NINA-LAMP), PLoS One 12 (2017) 1–15.
[16] Y.D. Ma, Y.S. Chen, G.B. Lee, An integrated self-driven microfluidic device for rapid detection of the Influenza A (H1N1) virus by reverse transcription loop-mediated isothermal amplification, Sensor. Actuator. B Chem. 296 (2019) 1–9.
[17] S. Vilcek, L. Strojny, B. Durkovic, W. Rossmanith, D. Paton, Storage of bovine viral samples on filter paper and detection of viral RNA by a RT-PCR method, J. Virol. Methods 92 (2001) 19–22.
[18] K.R. Daher, G. Stewart, M. Boissinot, M.G. Bergeron, Recombinase polymerase amplification for diagnostic applications, Clin. Chem. 62 (2016) 947–958.
[19] Y. Tang, X. Yu, H. Chen, Y.X. Diao, An immunoassay-based reverse-transcription loop-mediated isothermal amplification assay for the rapid detection of avian Influenza H5N1 virus viremia, Biosens. Bioelectron. 86 (2016) 255–261.
[20] C.H. Van-Den-Kieboom, S.L. Van-Der-Beek, T. Meszaros, R.E. Gyurcsanyi, G. Ferwerda, M.I. De-Jonge, Aptasensors for viral diagnostics, Trends Anal. Chem. 74 (2015) 58–67.
[21] S. Patra, R.G. Kerry, G.K. Maurya, B. Panigrahi, S. Kumari, J.R. Rout, Emerging molecular prospective of SARS-CoV-2: feasible nanotechnology based detection an inhibition, Front. Microbiol. 11 (2020) 1–23.
[22] M. Adiraj-Lyer, G. Oza, S. Velumani, A. Maldonado, J. Romero, M.D. Munoz, M. Sridharan, R. Asomoza, J.S. Yi, Scanning fluorescence-based ultrasensitive detection of dengue viral DNA on ZnO thin films, Sensor. Actuator. B Chem. 202 (2014) 1338–1348.
[23] C.E. Noguero, M.L. Valls, B. Sot, CRISPR/Cas technology as a promising weapon to combat viral infection, Bioessays 43 (2021) 1–16.
[24] X. Xie, T. Gjorgjieva, Z. Attieh, M.M. Dieng, M. Arnoux, M. Khair, Y. Moussa, F. A. Jaliaf, N. Rahiman, C.A. Jackson, L.E. Messery, K. Pampiona, Z. Victoria, M. Zafar, R. Ali, F. Piano, K.C. Gunsaius, Y. Idaghdour, Microfluidic nano-scale qPCR enables ultra-sensitive and quantitative detection of SARS-CoV-2, Process 8 (2020) 1–12.
[25] H.W. Xiong, X. Ye, Y. Li, X. Fang, J. Kong, Efficient microfluidic-based air sampling/monitoring platform for detection of aerosol SARS-CoV-2 on-site, Anal. Chem. 93 (2021) 4270–4276.
[26] M. Ji, Y. Xia, J.F.C. Loo, L. Li, H.P. Ho, J. He, D. Gu, Automated multiplex nucleic acid tests for rapid detection of SARS-CoV-2, Influenza A and B infection with direct reverse-transcription quantitative PCR (DirRT-qPCR) assay in a centrifugal microfluidic platform, RSC Adv. 10 (2020) 34088–34098.
[27] R.R.G. Soares, A.S. Akhtar, I.F. Pinto, N. Lapins, D. Barrett, G. Sandh, X. Yin, V. Pelechano, A. Russom, Sample-to-answer COVID-19 nucleic acid testing using a low-cost centrifugal microfluidic platform with bead-based signal enhancement and smartphone read-out, Lab Chip 21 (2021) 2932–2944.
[28] K.G. de Oliveria, P.F.N. Estrela, G. de Melo Mendes, C.A. dos Santos, E. de Paula Silveira Lacerda, G.R.M. Duarte, Rapid molecular diagnostics of COVID-19 by RT-LAMP in a centrifugal polystyrene-toner based microfluidic with end-point visual detection, Analyst 146 (2021) 1178–1187.
[29] A. Ganguli, A. Mostafa, J. Berger, M.Y. Aydin, F. Sun, S.A.S. de Ramirez, E. Valera, B.T. Cunningham, W.P. King, R. Bashir, Rapid isothermal amplification and portable detection system for SARS-CoV-2, Proc. Natl. Acad. Sci. U.S.A. 117 (2020) 22727–22735.
[30] B. Udugama, P. Kadhiresan, H.N. Kozlowski, A. Malekjahani, M. Osborne, V.Y. C. Li, H. Chen, S. Mubareka, J.B. Gubbay, W.C.W. Chan, Diagnosing COVID-19: the disease and tools for detection, ACS Nano 14 (2020) 3822–3835.
[31] C.H. Su, M.H. Tsai, C.Y. Lin, Y.D. Ma, C.H. Wang, Y.D. Chung, G.B. Lee, Dual aptamer assay for detection of acinetobacter baumannii on an electromagnetically-driven microfluidic platform, Biosens. Bioelectron. 159 (2020) 1–7.
[32] D.M. Dudley, C.M. Newman, A.M. Weiler, M.D. Ramuta, C.G. Shortreed, A. S. Heffron, M.A. Accola, W.M. Rehrauer, T.C. Friedrich, D.H. O'Connor, Optimizing direct RT-LAMP to direct transmissible SARS-CoV-2 from primary nasopharyngeal swab samples, PLoS One 15 (2020) 1–15.
[33] C.H. Weng, K.Y. Lien, S.Y. Yang, G.B. Lee, A suction-type, pneumatic microfluidic device for liquid transport and mixing, microfluid, Nanofluidics 10 (2010) 301–310.
[34] W.L. Wang, Y.L. Xu, R.Q. Gao, R.J. Lu, K. Han, G.Z. Wu, W.J. Tan, Detection of SARS-cov-2 in different types of clinical specimens, JAMA 323 (2020) 1843–1844.
[35] A. Ganguli, A. Mostafa, J. Berger, M.Y. Aydin, F. Sun, S.S. De-Ramirez, E. Valera, B. T. Cunningham, W.P. King, R. Bashir, Rapid isothermal amplification and portable detection system for SARS-CoV-2, Proc. Natl. Acad. Sci. U.S.A. 117 (2020) 22727–22735.
[36] J.N. Kanji, N. Zelyas, C. MacDonald, K. Pabbaraju, M.N. Khan, A. Prasad, J. Hu, M. Diggle, B.M. Berenger, G. Tipples, False negative rate of COVID-19 PCR testing: a discordant testing analysis, Virol. J. 18 (2021) 1–6.
[37] Y. Yang, M. Yang, C. Shen, F. Wang, J. Yuan, J. Li, M. Zhang, Z. Wang, L. Xing, J. Wei, L. Peng, G. Wong, H. Zheng, W. Wu, M. Liao, K. Feng, J. Li, Q. Yang, J. Zhao, Z. Zhang, L. Liu, Y. Liu, Evaluating the accuracy of different respiratory specimens in the laboratory diagnosis and monitoring the viral shedding of 2019-nCoV infections, medRxiv 2 (2020) 1–15.